

Crossover from 2D metal to 3D Dirac semimetal in metallic PtTe₂ films
with local Rashba effect

Ke Deng,^{1,*} Mingzhe Yan,^{1,*} Chu-Ping Yu,² Jiaheng Li,¹ Xue Zhou,¹ Kenan Zhang,¹
Yuxin Zhao,¹ Koji Miyamoto,³ Taichi Okuda,³ Wenhui Duan,^{1,4} Yang Wu,⁵ Xiaoyan
Zhong,² and Shuyun Zhou^{1,4,†}

¹*State Key Laboratory of Low Dimensional Quantum Physics and Department of Physics, Tsinghua University, Beijing 100084, China*

²*National Center for Electron Microscopy in Beijing, Key Laboratory of Advanced Materials (MOE), State Key Laboratory of New Ceramics and Fine Processing, School of Materials Science and Engineering, Tsinghua University, Beijing 100084, China*

³*Hiroshima Synchrotron Radiation Center, Hiroshima University, Higashi-Hiroshima 739-0046, Japan*

⁴*Collaborative Innovation Center of Quantum Matter, Beijing 100084, China*

⁵*Department of Physics and Tsinghua-Foxconn Nanotechnology Research Center, Tsinghua University, Beijing 100084, China*

*These authors contributed equally to this work.

†Correspondence should be sent to syzhou@mail.tsinghua.edu.cn

Abstract:

PtTe₂ and PtSe₂ with trigonal structure have attracted extensive research interests since the discovery of type-II Dirac fermions in the bulk crystals. The evolution of the electronic structure from bulk 3D topological semimetal to 2D atomic thin films is an important scientific question. While a transition from 3D type-II Dirac semimetal in the bulk to 2D semiconductor in monolayer (ML) film has been reported for PtSe₂, so far the evolution of electronic structure of atomically thin PtTe₂ films still remains unexplored. Here we report a systematic angle-resolved photoemission spectroscopy (ARPES) study of the electronic structure of high quality PtTe₂ films grown by molecular beam epitaxy with thickness from 2 ML to 6 ML. ARPES measurements show that PtTe₂ films still remain metallic even down to 2 ML thickness, which is in sharp contrast to the semiconducting property of few layer PtSe₂ film. Moreover, a transition from 2D metal to 3D type-II Dirac semimetal occurs at film thickness of 4–6 ML. In addition, Spin-ARPES measurements reveal helical spin textures induced by local Rashba effect in the bulk PtTe₂ crystal, suggesting that similar hidden spin is also expected in few monolayer PtTe₂ films. Our work reveals the transition from 2D metal to 3D topological semimetal and provides new opportunities for investigating metallic 2D films with local Rashba effect.

Keywords: PtTe₂, Dirac semimetal, local Rashba effect, topological semimetal, topological superconductivity

1. Introduction

Transition metal dichalcogenides (TMDCs) are fascinating layered materials with rich physics and potential applications [1-3]. Among the large family of compounds, group-10 TMDCs (PtS₂, PtTe₂ and PtSe₂) with trigonal (1T) structure have distinctive properties, yet they remain least investigated until recent years [4-8]. In contrast to semiconducting group-6 TMDCs (e.g. MoS₂) which usually forms thermodynamically stable hexagonal (2H) structure, platinum ditelluride (PtTe₂) crystalizes in trigonal structure and early band structure calculation suggests that the bulk crystal is a metal [9]. Recently, bulk PtTe₂ crystal has been reported to host nontrivial topological type-II Dirac fermions, and massless Dirac fermions are found to emerge at the topologically protected touching points of electron and hole pockets [6]. The strongly tilted Dirac cone along the out-of-plane momentum direction breaks the Lorentz invariance and therefore provides the counterpart beyond standard model of physics [10]. The isostructural material PtSe₂ is also a type-II Dirac semimetal [11,12], and shows metal-semiconductor transition with decreasing thickness [4, 13, 14]. In addition, monolayer PtSe₂ shows interesting helical spin texture [8] induced by local Rashba effect (R-2) [15] despite the fact that the monolayer film itself is centrosymmetric. Such hidden spin texture induced by local Rashba effect has been predicted to provide an important platform for realizing novel topological superconductivity with odd parity if s-wave superconducting pairing can be added [16-18]. Theoretically it has been proposed that

carrier doping on PtSe₂ can tune the electron-phonon interaction and enhance the strength of superconductivity [19]. However, considering that PtSe₂ is a semiconductor with a large gap size of ≈ 1.2 eV [4], it is difficult to tune the Fermi energy in such a large range to make it a superconductor. Finding a similar centrosymmetric film with local Rashba effect yet with metallic property can provide a better opportunity for realizing topological superconductivity, and PtTe₂ is a good candidate considering that tellurides are usually more metallic than selenides.

Growth of PtTe₂ thin films with thickness down to a few nanometers has been reported by chemical vapor deposition (CVD) recently [20-22]. However, so far there is no report of thinner (sub-nanometer) films and the experimental electronic structure of PtTe₂ films still remains to be explored. In this work, we report a systematic angle-resolved photoemission spectroscopy (ARPES) study of the electronic structure of PtTe₂ films grown by molecular beam epitaxy (MBE) with controlled film thickness from 2 monolayers (ML) to 6 ML. ARPES measurements show that the PtTe₂ films remain metallic even down to the thinnest 2 ML, and there is a transition from 2D metallic film to 3D type-II Dirac semimetal at 4–6 ML. Spin-ARPES measurements reveal the spin texture induced by local Rashba effect in bulk PtTe₂ crystal. Considering that the local Rashba effect has been observed in bulk PtTe₂, PtSe₂ and monolayer PtSe₂, which all have similar crystal symmetry to PtTe₂ films, we expect PtTe₂ films to exhibit similar local Rashba effect. Therefore, atomically thin PtTe₂ film is an interesting metallic film with local Rashba effect, which is compatible with requirements for the new mechanism of topological superconductivity [16].

2. Method

Atomically thin PtTe₂ films with different thickness from 2 ML to 6 ML were grown on bilayer graphene/6H-SiC (0001) in the ultra-high vacuum (UHV) system with a base pressure of 2×10^{-10} torr. The graphene was grown by flash annealing the 6H-SiC substrate at 1,350 °C [23]. The growth process is monitored by high energy electron diffraction (RHEED). After 60 cycles of flash annealing process, sharp diffraction pattern from graphene is observed in low energy electron diffraction (LEED) (Fig. 1c) and RHEED (Fig. 1e). High purity Pt (Alfa Aesar, 99.95%) and Te (Alfa Aesar, 99.999%) were then evaporated onto the substrate at 300 °C with the flux ratio of 20:1 to ensure a Te rich environment. After the film growth, in situ annealing process was employed to improve the film quality, and the Te flux was maintained during the annealing process to avoid Te vacancies in the sample. The as-grown PtTe₂ films with different thickness were then transferred to angle-resolved photoemission spectroscopy (ARPES) chamber for in situ ARPES measurements, or capped with Te protection layer before taking out for TEM measurements. ARPES measurements were performed at 80 K using helium lamp (21.2 eV) source. Spin-ARPES measurements of PtTe₂ bulk crystal were performed at ESPRESSO endstation of Hiroshima Synchrotron Radiation Center at temperature of 20 K using Helium lamp.

First-principle calculations were carried out by the Vienna ab initio Simulation Package (VASP) [24] in the framework of density functional theory, with the projector

augmented wave (PAW) methods and the Perdew-Burke-Ernzerhof-type generalized gradient approximation (GGA). The kinetic energy cutoff used in the whole calculations is fixed at 400 eV, and the DFT-D3 method is included to correct van der Waals interaction of layered PtTe_2 . The spin-orbit coupling effect is included self-consistently. The k -point mesh grid of $12 \times 12 \times 6$ is taken for bulk calculations, and $12 \times 12 \times 1$ for multi-layer thin films. The lattice constants are fixed at experimental data, and all the atomic positions are fully relaxed with the force criteria of 0.01 eV/\AA .

3. Results and discussion

PtTe_2 crystallizes in trigonal structure (see top and side views in Fig. 1a), corresponding to CdI_2 -type structure with $P\bar{3}m1$ space group. Sharp diffraction pattern from the PtTe_2 film is observed both in LEED and RHEED (Fig. 1d,f) after PtTe_2 film growth, indicating the high quality of the film. The crystal structure of PtTe_2 film is revealed by transmission electron microscopy (TEM) measurements in Fig. 1g. The high quality MBE PtTe_2 films with controllable thickness down to 2 ML provide a unique opportunity for a systematic study of the electronic structure as a function of film thickness.

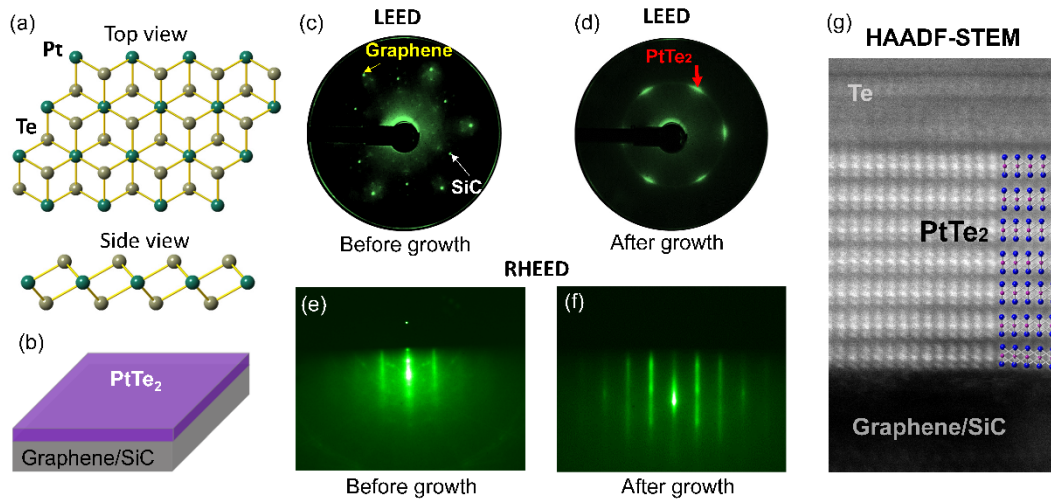


Fig.1. Crystal structure of 1T- PtTe_2 film. (a) Top and side views of PtTe_2 . Each monolayer is defined as one PtTe_2 sandwiched block. (b) An illustration of PtTe_2 grown on bilayer graphene/6H-SiC (0001). (c, d) LEED patterns of sample before (c) and after (d) growth respectively. (e, f) RHEED patterns taken before (e) and after (f) PtTe_2 film growth respectively. (g) HAADF-STEM image of a sample cross section. Te atoms were capped over the sample surface to protect it from degradation.

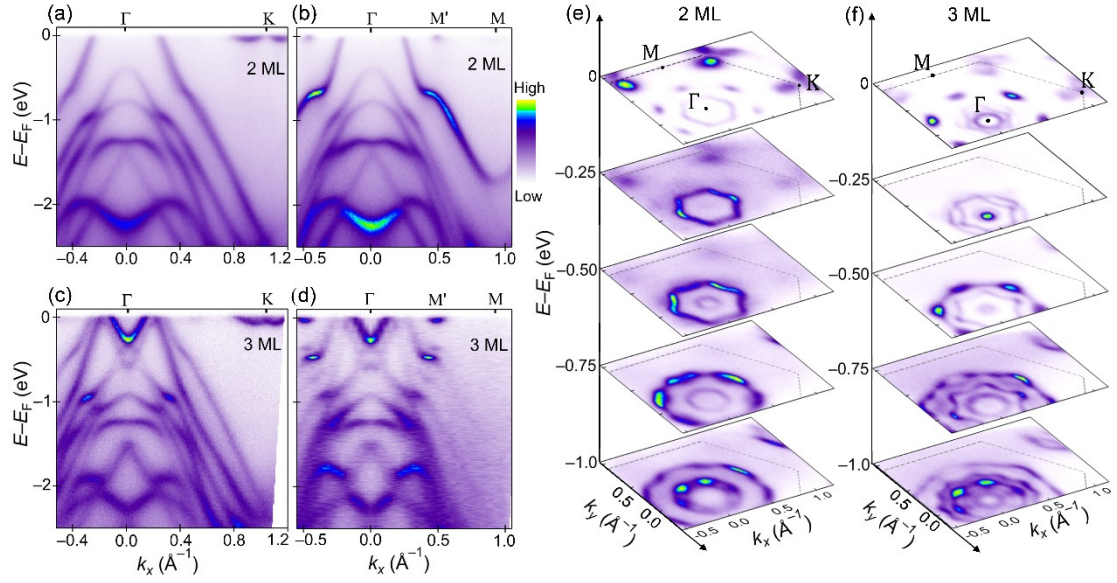


Fig. 2. The electronic structure of 2 ML and 3 ML PtTe₂ films (a, b) ARPES spectra of 2 ML PtTe₂ film along the $\Gamma - K$ and $\Gamma - M$ directions, respectively. (c, d) ARPES spectra of 3 ML PtTe₂ film along the $\Gamma - K$ and $\Gamma - M$ directions, respectively. (e, f) Intensity maps measured at energies from E_F to -1.0 eV.

Fig. 2 shows the electronic structures of 2 ML and 3 ML PtTe₂ films measured by ARPES. Fig. 2a–d shows the dispersions for 2 ML and 3 ML films along two high symmetry directions, $\Gamma - K$ and $\Gamma - M$ direction respectively. For 2 ML film, the dispersion shows a hole pocket centered at the Γ point near the Fermi energy (E_F), and two electron pockets near the K point. Along the $\Gamma - M$ direction, another electron pocket is observed at the mid-point (labeled as M') between the Γ and M points. Such pocket is observed as gapped Dirac cone in bulk PtTe₂ [6]. The electronic structure shows that the 2 ML film is metallic, which is in sharp contrast to PtSe₂ films [13]. For 3 ML film, the pocket at the Γ point splits into two, and there are more bands at high binding energies as well. In addition, there are two electron pockets centered at the Γ point. Fig. 2e, f shows the intensity maps at selected energies from E_F to -1 eV measured for both 2 ML and 3 ML films. The electron pocket at the Γ point shows a hexagonal shape at E_F and it expands in size with binding energy in 2 ML sample. Below -0.5 eV, another pocket starts to appear at the Γ point and it expands in size with energy too. In addition, there are electron pockets around the K point and the M' point at E_F . For 3 ML film, there are four electron pockets at E_F and they become more obvious at -0.25 eV, and the pockets near the K and M' points are similar to those in 2 ML film. The ARPES measurements show that unlike its isostructural PtSe₂ films that show metal-semiconductor transition with decreasing film thickness [4, 13], PtTe₂ films, however, remain metallic even down to 2 ML. First principle calculations show that 1 ML PtTe₂ is semiconductor [25–27], which still awaits further experimental verification.

To reveal the evolution from 2D metal film to 3D type-II Dirac semimetal, we show in Fig. 3 a systematical study of the band structure of PtTe₂ films from 2 ML to 6 ML

and the bulk crystal along the $\Gamma - K$ direction. There are two interesting conical dispersions and we can follow their evolution with sample thickness. First of all, from 2 ML to 3 ML, two V-shaped pockets (marked by red arrow in Fig. 3b) emerge at E_F at the Γ point. The V-shaped pockets move down in energies and eventually touch the hole-like pocket at higher binding energy, resulting in three-dimensional type-II Dirac fermions in the bulk (Fig. 3e) [6]. We note that the 4 ML and 6 ML films show similar dispersion to the bulk crystal, and this suggests that they effectively have the bulk property of the topological semimetal. The thickness dependent ARPES data allow to follow the evolution of the valence band and reveal the transition from a 2D metal to a 3D topological semimetal at thickness of 4–6 ML. The other conical dispersion is at higher energy from -2 to -3 eV (grey arrows). For 2 ML film, there is a gap between the rounded M-shaped and W-shaped dispersions between -2 and -3 eV. These two bands become closer in 3 ML film and they merge to form a Dirac cone in 4 ML and 6 ML films. This Dirac cone is the topological surface state, similar to that reported in PtSe₂ [6] and PdTe₂ [28]. First principles calculation (dotted curves in Fig. 3f–j) shows dispersions in agreement with ARPES results, supporting the transition from 2D metallic film to 3D type-II Dirac semimetal at 4–6 ML.

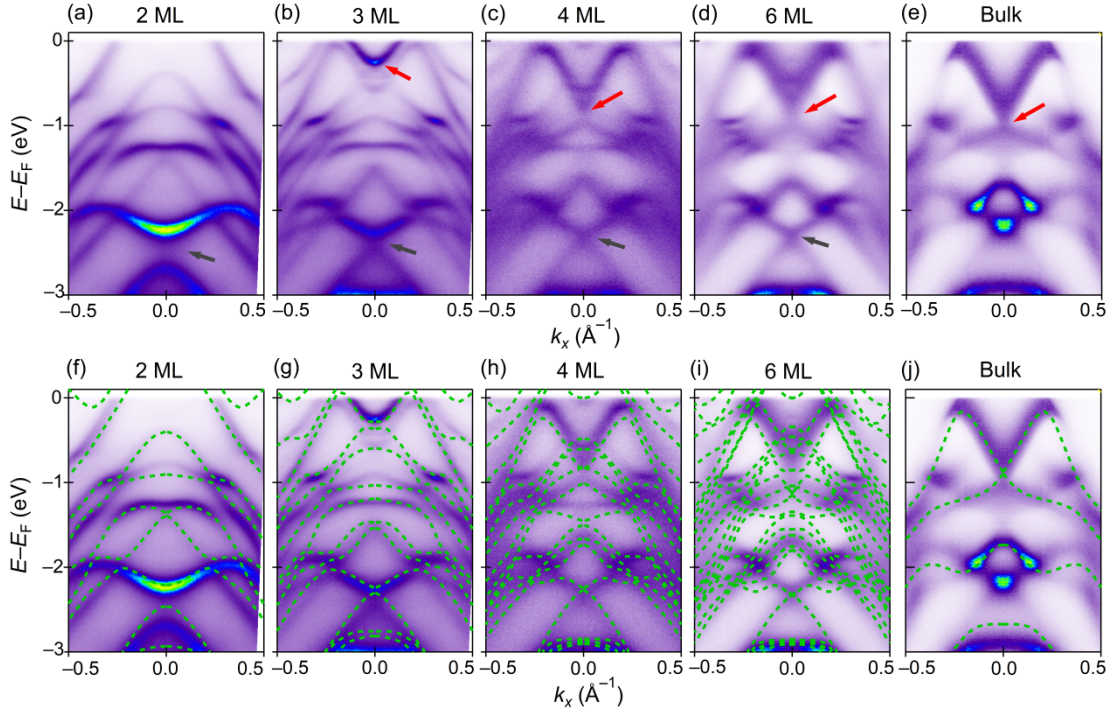


Fig. 3. Evolution of the electronic structure of PtTe₂ films from 2D metal to 3D type-II Dirac semimetal. (a–e) Measured ARPES spectra of PtTe₂ films with different thickness from 2 ML to 6 ML and the bulk crystal along the $\Gamma - K$ direction. (f–j) Comparison of measured ARPES dispersions with calculated band structures (green dotted lines) along the $\Gamma - K$ direction.

Considering that PtTe₂ and PtSe₂ have similar crystal structure, and that helical spin texture is observed both in monolayer PtSe₂ film [8] and bulk PtSe₂ [13] due to the local Rashba effect, we would expect similar spin physics also applies to bulk PtTe₂ and few layers of PtTe₂ films.

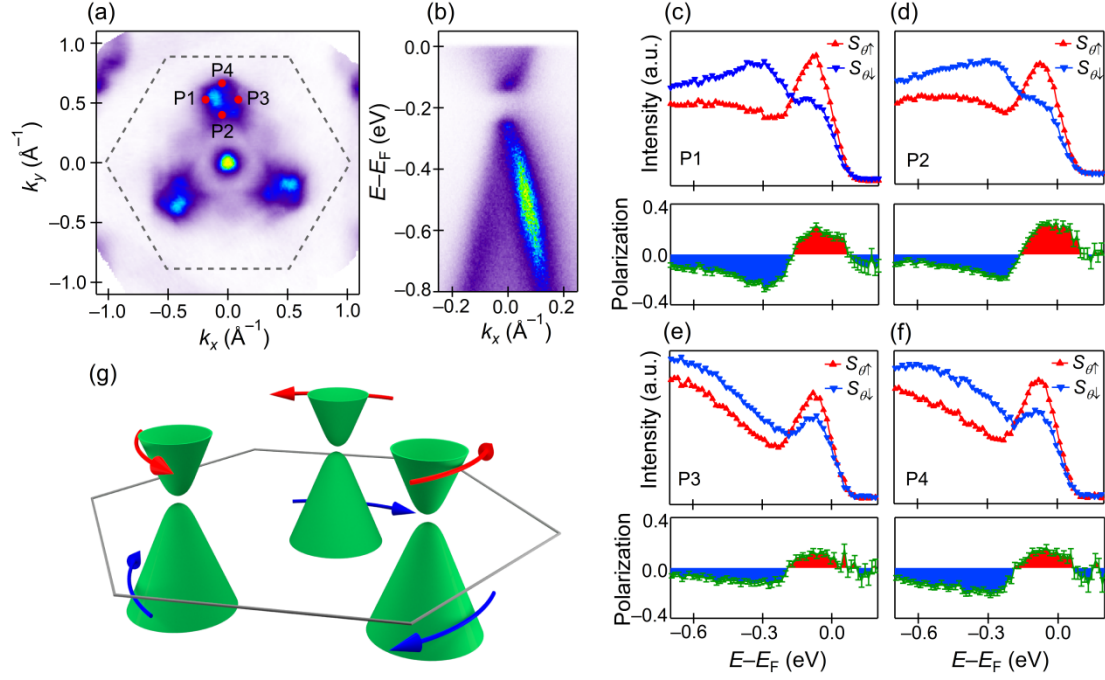


Fig.4. Helical spin texture for Dirac-like dispersion in the M' point of single crystal PtTe₂. (a) Intensity map measured at -0.6 eV. Red dots mark the measurement position P1–P4 for EDCs shown in (c–f). (b) Measured dispersion of the gapped Dirac-like dispersion at photon energy of 21.2 eV. (c–f) Spin-resolved EDCs for the in-plane tangential direction from P1–P4. (g) A schematic plot of the spin texture of the gapped Dirac-like dispersion.

In Fig. 4, we reveal the helical spin texture for bulk PtTe₂ crystal. Fig. 4a shows the intensity map of PtTe₂ at -0.6 eV and a pocket is observed at the M' point. The dispersion of this pocket shows a gapped Dirac-like dispersion (Fig. 4b). Fig. 4c–f shows the spin contrast of energy distribution curves (EDCs) along the in-plane tangential direction at four selected momentum points on this pocket (P1 to P4). A large spin contrast is observed along the tangential direction (θ) for all EDCs. While the lower part of Dirac-like dispersion shows spin-down at all points measured (P1–P4), the upper cone is spin-up with strong polarization. Fig. 4g shows an illustrative figure of the observed spin polarization. Here all these points on the same Dirac-like dispersion at the M' point show spin polarization along the tangential direction with respect to Γ point. Considering the three-fold rotational symmetry of the crystal, the spin polarization of these three cones at the three equivalents M' points forms a helical spin texture with respect to the Γ point. Such in-plane tangential helical spin texture can be explained by the local dipole field between the Pt and Te atoms, similar to the case of PtSe₂ [8, 13]. Since the crystal symmetry of the bulk PtTe₂ is the same as atomically thin PtTe₂ films, the PtTe₂ films from 2 ML to 6 ML are also expected to

have similar local Rashba effect and similar spin texture. Similar hidden spin polarization has also been predicted in other 1T films [29], which still awaits further experimental verification. Here we show that atomically thin PtTe₂ is metallic with local Rashba effect, and can be tuned to 3D Dirac fermions by increasing the film thickness.

4. Conclusions

In summary, we have successfully grown atomically thin PtTe₂ films with controlled thickness and revealed the evolution of the electronic structure with film thickness. Our ARPES results show that even the 2 ML PtTe₂ film is metallic, which is in contrast to semiconducting PtSe₂. Moreover, a systematic study shows that the PtTe₂ film evolves from a 2D metallic film to a 3D Dirac semimetal at 4–6 ML thickness. In addition, we report helical spin texture induced by the local Rashba effect in bulk PtTe₂, which also holds in atomically thin metallic PtTe₂ films (including 2 ML, 4 ML to 6 ML films) due to the same crystal structure. Metallic PtTe₂ thin films with local Rashba effect, can serve as a new platform to investigate topological superconductivity. Our work reveals the novel physics in PtTe₂ and paves the way for further investigation.

Conflict of interest

The authors declare that they have no conflict of interests.

Acknowledgments

This work was supported by the National Natural Science Foundation of China (11725418 and 11334006), Ministry of Science and Technology of China (2016YFA0301004, 2016YFA0301001, and 2015CB921001), Science Challenge Project (TZ2016004) and Beijing Advanced Innovation Center for Future Chip (ICFC). Spin-ARPES experiments at Hiroshima Synchrotron Radiation Center have been performed under the proposal number 14-A-15 and 16AG058.

Author contributions

SZ conceived the research project. MY, XZ and YZ grew and characterized the thin film samples, KZ grew the PtTe₂ single crystal with support from YW. MY, XZ, YZ, KZ and KD performed the ARPES measurements and analyzed the data. ZY and XYZ performed the TEM measurements. JL and WD performed first-principle calculations. KD, MY and SZ wrote the manuscript, and all authors commented on the manuscript.

References

- [1] Wang Q H, Kalantar-Zadeh K, Kis A, et al. Electronics and optoelectronics of two-dimensional transition metal dichalcogenides. *Nat Nanotechnol* 2012; 7, 699.
- [2] Chhowalla M, Shin H S, Eda G, et al. The chemistry of two-dimensional layered transition metal dichalcogenide nanosheets. *Nat Chem* 2013; 5: 263.
- [3] Manzeli S, Ovchinnikov D, Pasquier D, et al. 2D transition metal dichalcogenides. *Nat Rev Mater* 2017; 2: 17033
- [4] Wang Y, Li L, Yao W, et al. Monolayer PtSe₂, a new semiconducting Transition-Metal-Dichalcogenide, epitaxially grown by direct selenization of Pt. *Nano Lett* 2015; 15, 4013.
- [5] Zhao Y, Qiao J, Yu P et al. Extraordinarily strong interlayer interaction in 2D layered PtS₂. *Adv Mater* 2016; 28, 2399.
- [6] Yan M, Huang H, Zhang K, et al. Lorentz-violating type-II Dirac fermions in transition metal dichalcogenide PtTe₂. *Nat Commun* 2016; 8, 257.
- [7] Zhao Y, Qiao J, Yu Z et al. High-electro-mobility and air-stable 2D layered PtSe₂ FETs. *Adv Mater* 2017; 29, 1604230.
- [8] Yao W, Wang E, Huang H, et al. Direct observation of local Rashba spin polarization and spin-layer locking in centrosymmetric monolayer PtSe₂. *Nat Commun* 2017; 8, 14216.
- [9] Orders P J, Liesegang J, Leckey R C G, et al. Angle-resolved photoemission from the valence bands of NiTe₂, PdTe₂ and PtTe₂. *J Phys F: Met Phys*, 1982; 12,2737.
- [10] Soluyanov A A, Gresch D, Wang Z, Wu Q et al. Type-II Weyl semimetals. *Nature* 2015; 527, 495.
- [11] Huang H, Zhou S, Duan W. Type-II Dirac fermions in the transition metal dichalcogenide PtSe₂ class. *Phys Rev B* 2016; 94, 121117(R)
- [12] Zhang K, Yan M, Zhou X, et al. Experimental evidence of type-II Dirac fermions in PtSe₂. *Phys Rev B* 2017; 96,125102.
- [13] Yan M, Wang E, Zhou X, et al. High quality atomically thin PtSe₂ films grown by molecular beam epitaxy. *2D Mater* 2017; 4, 045015.
- [14] Ciarrocchi A, Avsar A, Ovchinnikov D, et al. Thickness-modulated metal-to-semiconductor transformation in a transition metal dichalcogenide. *Nat Commun* 2018; 9, 919.
- [15] Zhang X, Liu Q, Luo, J et al. Hidden spin polarization in inversion-symmetric bulk crystals. *Nat Phys* 2014; 10: 387.
- [16] Nakosai S, Tanaka Y, Nagaosa N. Topological superconductivity in bilayer Rashba system. *Phys Rev Lett* 2012; 108: 147003.
- [17] Liu C X. Unconventional superconductivity in bilayer transition metal dichalcogenides. *Phys Rev Lett* 2017; 118: 087001.
- [18] Nakamura Y, Yanase Y. Odd-parity superconductivity in bilayer transition metal dichalcogenides. *Phys Rev B* 2017; 96: 054501.
- [19] Cheng C, Sun J T, Liu M, et al. Tunable electron-phonon coupling superconductivity in platinum diselenide. *Phys Rev Mater* 2017; 1: 074804.
- [20] Fu L, Hu D, Mendes R G, et al. Highly organized epitaxy of Dirac semimetallic PtTe₂ crystals with extrahigh conductivity and visible surface plasmons at edges. *ACS Nano* 2018; 12:9405-9411.

- [21] Ma H, Chen P, Li B, et al. Thickness-tunable synthesis of ultrathin type-II Dirac semimetal PtTe₂ single crystals and their thickness-dependent electronic properties. *Nano Lett* 2018; 18: 3523-3529.
- [22] Hao S, Zeng J, Xu T, et al. Low-temperature eutectic synthesis of PtTe₂ with weak antilocalization and controlled layer thinning. *Adv Funct Mater* 2018; 28: 1803746.
- [23] Wang Q, Zhang W, Wang L, et al. Large-scale uniform bilayer graphene prepared by vacuum graphitization of 6H-SiC (0001) substrates. *J Phys: Condens Matter*, 2013; 25: 095002.
- [24] Kresse G, Furthmüller J. Efficient iterative schemes for ab initio total-energy calculations using a plane-wave basis set. *Phys Rev B* 1996; 54, 11169.
- [25] Du J, Song P, Fang L, et al. Elastic, electronic and optical properties of the two-dimensional PtX₂ (X= S, Se, and Te) monolayer. *App Surf Sci*, 2018; 435, 476-482
- [26] Zhuang H L, Hennig R G. Computational search for single-layer transition-metal dichalcogenide photocatalysts. *J Phys Chem C*, 2013; 117: 20440-20445
- [27] Rasmussen F A, Thygesen K S. Computational 2D materials database: electronic structure of transition-metal dichalcogenides and oxides. *J Phys Chem C*, 2015; 119: 13169-13183
- [28] Yan L, Jian-Zhou Z, Li Y, et al. Identification of topological surface state in PdTe₂ superconductor by angle-resolved photoemission spectroscopy. *Chin Phys Lett* 2015; 32, 067303
- [29] Cheng C, Sun J T, Chen X R, et al. Hidden spin polarization in the 1T-phase layered transition-metal dichalcogenides MX₂ (M= Zr, Hf; X= S, Se, Te). *Sci Bull* 2018; 63: 85-91